Velocity statistics of the Nagel-Schreckenberg model

Nicolas Bain,[*] Thorsten Emig,[†] and Franz-Josef Ulm[‡]

Multi-Scale Materials Science for Energy and Environment, ⟨MSE⟩², UMI 3466, The Joint CNRS-MIT Laboratory,
Massachusetts Institute of Technology, 77 Massachusetts Avenue, Cambridge, Massachusetts 02139, USA

Michael Schreckenberg[§]

Physik von Transport und Verkehr, Universität Duisburg-Essen, 47048 Duisburg, Germany

The statistics of velocities in the cellular automaton model of Nagel and Schreckenberg for traffic are studied. From numerical simulations, we obtain the probability distribution function (PDF) for vehicle velocities and the velocity-velocity (vv) covariance function. We identify the probability to find a standing vehicle as a potential order parameter that signals nicely the transition between free congested flow for a sufficiently large number of velocity states. Our results for the vv covariance function resemble features of a second-order phase transition. We develop a 3-body approximation that allows us to relate the PDFs for velocities and headways. Using this relation, an approximation to the velocity PDF is obtained from the headway PDF observed in simulations. We find a remarkable agreement between this approximation and the velocity PDF obtained from simulations.

I. INTRODUCTION

Traffic flow theory is the backbone for understanding and improving the mobility of people and goods in our road networks. The classical tool to characterizing mobility (in either field tests or from simulations) is by plotting flow vs density in the form of the so-called fundamental diagram (Fig. 1) for both individual road segments and road networks [1], to separate free flow patterns below a critical density from congested flow patterns above. While empirical approaches based on equilibrium concepts link vehicle speed to density, eventually enriched by information related to human behavior [2], the fundamental structure of the transition from free to congested flow remains a topical issue, which may ultimately reconcile the considerable scatter in field experiments with traffic flow theory and simulation. This provides ample motivation for us to study velocity distribution functions of a specific class of traffic models, cellular automata models (CA), which are known to exhibit two different phases (free and congested flow) and a transition between them [3]. Specifically, we herein investigate the velocity distribution functions for a simple version of these models, namely, the Nagel-Schreckenberg (NaSch) model for one-lane traffic [4]. The model is based on the discretization of the road into cells of the size of a single vehicle, and the whole system is described as the ensemble $(v_1,\ldots,v_N,d_1,\ldots,d_N)$ of velocities v_j and headways d_j (number of empty cells in front of a vehicle) of N vehicles [4,5]. The time evolution of the vehicle positions x_j and velocities v_j follows four distinct update rules:

(1) Acceleration: $v_j = \min(v_j + 1, v_{\max})$,

(2) Deceleration: $v_j = \min(d_j, v_j)$,

(3) Random deceleration: $v_j = \max(v_j - 1, 0)$ with a probability p,

(4) Movement: $x_j \to x_j + v_j$.

Herein, the velocity $v_{\max}$, a model parameter, corresponds to the maximum velocity that a vehicle can reach when there are no slower vehicles ahead. The stochastic parameter p represents the probability that a vehicle randomly slows down, and aims at capturing the lack of perfection in human behavior. In practice, the parameters $v_{\max}$ and p are kept constant, while the total density of vehicles ρ is varied, which is the number of vehicles divided by the number of cells. For convenience, the physical dimensions of headway and vehicle position are expressed in units of cells, and the velocity in units of cells per iteration time step; thus omitting the time dimension so that velocities and distances have formally the same dimension.

The NaSch model has been studied through mean-field (MF) theories for which velocity distribution functions were computed [5]. Since MF theories fail to give simple and accurate results for values of $v_{\max} > 2$, our study of the probability distribution function (PDF) for velocities of the NaSch model is based on both numerical simulations and exact results for a simplified 3-body approximation. To obtain the PDF, we analyze in detail the $v_{\max} + 1$ different accessible single-vehicle velocity states between 0 and $v_{\max}$. We choose a value of $v_{\max} = 10$ which ensures obtaining a sufficiently large number of states, and which is of the order of magnitude of typical highway speeds. The stochastic parameter is chosen to be $p = 0.5$ and remains constant throughout the study, as well as $v_{\max}$, except when mentioned otherwise. In order to avoid finite size effects we run simulations with periodic boundary conditions over 2×10^4 cells for 10^6 iteration time steps after a warm up time of 10^5 time steps to reduce the influence of transient behavior. With this choice of parameters, the number of vehicles used in our simulations range in $N \in [200; 8100]$. To probe the effect of different initial conditions we initialized the system in three distinct ways:

(I1) Megajam: block of N standing vehicles [3],

(I2) Equally spaced, standing vehicles [6],

(I3) Equally spaced vehicles moving with $v_{\max}$.

Our results turned out to be independent of these initial conditions, which ensures us that the warm-up time is sufficiently

[*]nbain@mit.edu

[†]emig@mit.edu

[‡]ulm@mit.edu

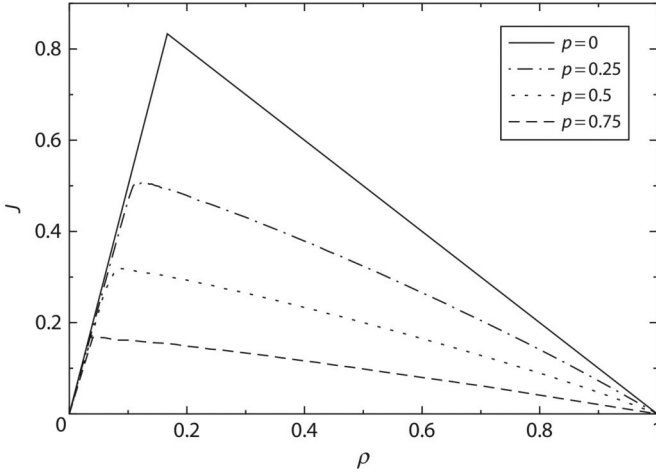[§]michael.schreckenberg@uni-due.de

FIG. 1. Numerically obtained fundamental diagrams of the NaSch model with $v_{\max} = 5$ for different values of the stochastic parameter p. (Flow j is in arbitrary units.) Taken from Ref. [1].

high. The results were also checked to be independent of the number of cells and the number of time steps.

As already noted, the NaSch model exhibits two different phases (free and congested flow) and a transition between them with a yet to be defined order parameter [1]. Specifically, in the deterministic case ($p = 0$), a sharp phase transition occurs at a critical density $\rho_c = 1/(v_{\max} + 1)$ that coincides with the density of maximum flow $j = \rho\langle v \rangle$, where $\langle v \rangle$ is the mean velocity of all vehicles, averaged over time. It has been a subject of intense debate in recent literature if the NaSch model exhibits a similar sharp transition in the presence of randomness ($p > 0$). In Sec. II we shed new light on this still open key question by analyzing the statistics of velocities. We identify an approximate "order parameter," and study the "transition" by looking at the velocity-velocity covariance function. In Sec. III we show that the PDF for velocities and headways cannot be obtained straightforwardly from the parameters of the model since there are no separate PDFs in the free and jammed flow. Based on the insight thus gained, we develop, in Sec. IV, an exact solution for a 3-body approximation. This approximation is employed in Sec. V to provide estimates of the velocity PDF from the knowledge of the PDF for headways. The paper concludes with a summary and discussion of our findings.

II. POTENTIAL "ORDER PARAMETER" AND VELOCITY CORRELATIONS

The NaSch model with randomness exhibits some kind of transition when going from low to high densities. Below the transition, there exists a free flow regime in which the interactions between vehicles are negligible and the flow j increases linearly with density. Above the transition, one encounters a congested regime in which the flow j decreases with increasing density. The flow-density relation, usually referred to as fundamental diagram, hence clearly shows a transition. Examples for the NaSch model for $v_{\max} = 5$ and different values of the stochastic parameter p are shown in Fig. 1. One might expect the existence of a genuine phase
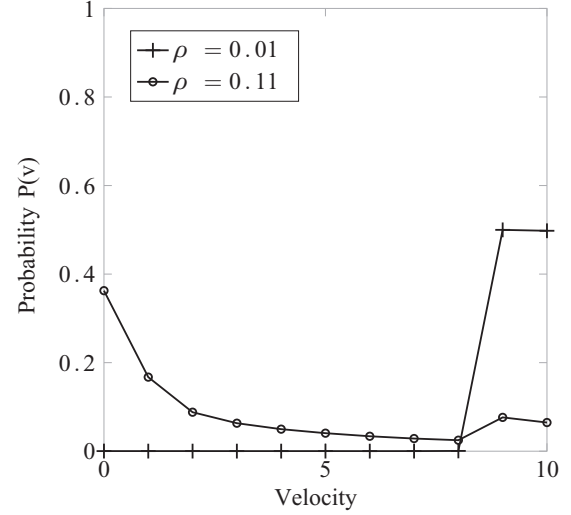

FIG. 2. Velocity PDFs in both the free and congested flow phases. The PDF for freely flowing vehicles is nonzero only for $v_{\max}$ with value $1 - p$ and $v_{\max} - 1$ with value p. In the congested regime the probability of finding a standing vehicle is finite, signaling the presence of traffic jams.

transition but it is not straightforward to define a corresponding order parameter because it is not obvious what symmetry is broken at the transition. To address this point, we inspect the PDF for velocities, $P(v)$. Averaging over all simulation time steps, we find two very distinct distributions in the two phases (Fig. 2). In the free flow phase, the vehicles do not interact and every vehicle can travel either at velocity $v_{\max}$ or $v_{\max} - 1$ with some negligible interactions. This solution is exactly known from the update rules, from taking the limit $d_j > v_{\max}$. In the congested phase the probability of finding a standing vehicle is strictly nonzero, $P(v = 0) > 0$, and the probability of having a vehicle at velocity $v_{\max}$ or $v_{\max} - 1$ decays with increasing density. The numerical result for $P(v = 0)$ as a function of density is shown in Fig. 3. The curve shows a clear drop to zero at a density $\rho_c \approx 0.036$. This suggests that $P(v = 0)$ could be an order parameter for a putative phase transition between free and congested flow. However, it has been argued in Ref. [3] that for small densities $\rho \to 0$ one has the scaling $P(v = 0) \sim \rho^{v_{\max}-1}$ showing that $P(v = 0)$ is nonzero at *any* density, and hence cannot serve as an order parameter in general. This can be reconciled with our observation for $v_{\max} = 10$ by studying the behavior of $P(v = 0)$ for smaller $v_{\max}$ which is shown in the insets of Fig. 3. While for $v_{\max} = 2$ there is indeed a continuous variation of $P(v = 0)$ with a change of curvature close to the critical density (density of maximum flow) found in Ref. [3], already for $v_{\max} = 5$ there is a rather steep drop in $P(v = 0)$ very close to the critical density in Ref. [3]; see also Fig. 1 for $p = 0.5$.

Our observations suggest that $P(v = 0)$ can be considered as an approximate or effective order parameter that describes the transition rather well for sufficiently large $v_{\max}$. We argue that in a continuum version of the NaSch model with an infinite number $v_{\max} \to \infty$ of discrete velocity states, $P(v = 0)$ becomes a genuine order parameter. This order parameter is different from previously adopted choices such as the number of vehicles in the high local density phases [7], the density of
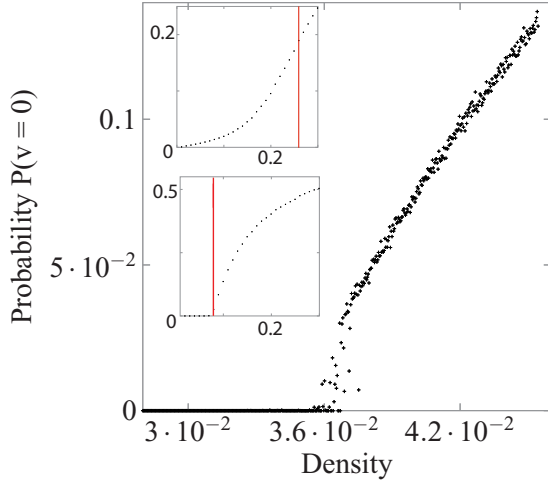
FIG. 3. Probability to find a standing vehicle, $P(v = 0)$, as function of the average density, for a system initialized with equally spaced, standing vehicles, and $v_{\max} = 10$. Every dot corresponds to a full simulation at constant density. The critical density is close to $\rho_c = 0.036$. Insets: $P(v = 0)$ for $v_{\max} = 2$ (top) and $v_{\max} = 5$ (bottom) with the critical densities obtained numerically in Ref. [3] marked by vertical lines.

nearest-neighbor pairs at rest [2], or the deviation of the mean velocity from the velocity of free-moving vehicles [3]. The data for $P(v = 0)$ extremely close to the critical density are the only ones in our numerical study that very slightly depend on the initial conditions, presumably due to the vicinity to the critical density. However, the results for $v_{\max} = 10$ always show a discontinuity around ρ_c. The behavior could be an artefact of finite simulation time, but this problem seems unavoidable because of the divergence of the time needed to reach a steady state close to ρ_c [3].

To gain a better understanding of the system's behavior at the transition, we study the velocity-velocity covariance function

$$G_v(r) = \frac{1}{NT} \sum_{t=1}^{T} \sum_{j=1}^{N} v_j(t) v_{j+r}(t) - \langle v \rangle^2, \quad (1)$$

where T is the simulation time, whereas $\langle v \rangle$ denotes the average, over time and vehicles, of the individual vehicle velocities $v_j(t)$ at time step t:

$$\langle v \rangle = \frac{1}{NT} \sum_{j=1}^{N} \sum_{t=1}^{T} v_j(t). \quad (2)$$

We observe, in Fig. 4, three distinct behaviors of the velocity-velocity covariance function: (1) Well below the critical density, at $\rho = 0.01$, we find no correlation in the velocity of successive vehicles [Fig. 4(a)]. This is consistent with a free flow in which all vehicles behave independently from each another. (2) Well above the critical point, at $\rho = 0.21$, [Fig. 4(c)], we observe an exponential decay with a correlation number of $r_c \approx 4$ successive vehicles [Fig. 4(d)] which is characteristic of short-range correlations. (3) Just above the critical density, at $\rho = 0.05$, we find a nearly linear decay of the covariance function, suggesting a diverging correlation number r_c [Fig. 4(b)].
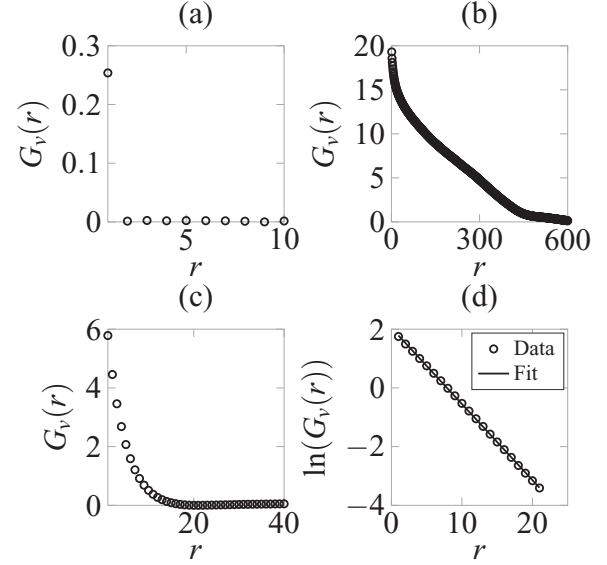

FIG. 4. Velocity-velocity covariance function [see Eq. (1)] as a function of the vehicle number r in the free flow regime (a), just above the critical density ρ_c (b), and well above the critical density (c). Shown in (d) is also a logarithmic plot of the velocity-velocity covariance function well above the critical density fitted with a line corresponding to a correlation number $r_c \approx 4$.

This divergence of the correlation number close to the critical density mimics a second-order phase transition.

III. PDF OF VELOCITIES

The PDF of the velocities, as shown in Fig. 2, might suggest that the PDFs for velocities and headways could be computed as the sum of a PDF for the jammed phase (P_J and Q_J, respectively) and a PDF for free flow phase (P_F and Q_F, respectively), weighted by the proportion of the number of vehicles in each phase. This scheme has been proposed in Ref. [8]. When ω is the fraction of vehicles in the free flow phase, this superposition assumption yields the following PDF for velocities:

$$P(v) = \omega P_F(v) + (1 - \omega) P_J(v). \quad (3)$$

This form is convenient if one wants to predict velocity or headway PDFs from a given density. It is trivial to realize that when the traffic is solely in the free flow state, below the critical density ρ_c, the jammed headway distributions will differ at various densities since $\langle d \rangle = \rho^{-1}$. Therefore, to check the validity of this hypothesis, we numerically computed the headway and velocity PDFs at different densities within the range of coexistence of the free flow and congested states. Defining a jammed vehicle as a vehicle with velocity strictly smaller than $v_{\max} - 1$, we compared the obtained jammed PDFs at densities $\rho_1 = 0.08$, $\rho_2 = 0.15$, and $\rho_3 = 0.19$. The normalized differences between the velocity PDFs are shown in Fig. 5 and exhibit a minimal relative difference of the order of 10% between the different densities.

This observation shows that the superposition model expressed by Eq. (3) is but an oversimplification of the true behavior of the model. It suggests that the internal structure
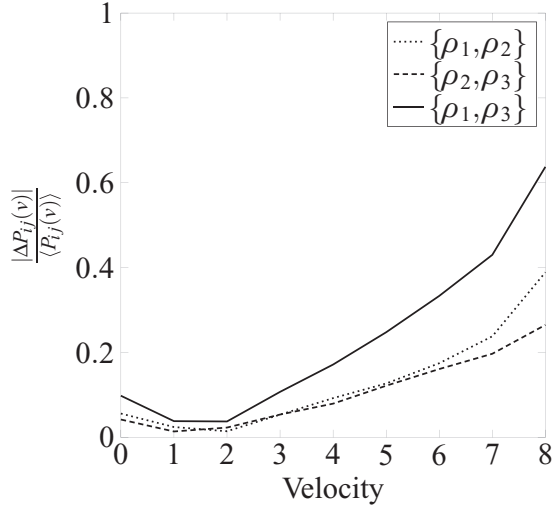
FIG. 5. Normalized velocity PDF differences with the notations $\Delta P_{ij}(v) = P_{\rho_i}(v) - P_{\rho_j}(v)$ and $\langle P_{ij}(v) \rangle = 0.5[P_{\rho_i}(v) + P_{\rho_j}(v)]$. The relative differences range from 10% to 60%, showing the need for a different approximation than Eq. (3).

of the traffic state quite certainly plays a role in the shape of the headway and velocity PDFs. One therefore needs a new method to predict velocity and headway distributions for the NaSch model.

IV. A 3-BODY APPROXIMATION: EXACT SOLUTION

We approach this problem analytically, by considering a 3-body approximation for the NaSch model for which an exact analytical solution is derived. To this end, consider a standing vehicle which we number as $j = 0$. Assume that this vehicle represents the tail of a jam and that it remains stopped. At a distance d_0 behind this vehicle we place a second vehicle, $j = 1$, and a third one, $j = 2$, in the cell immediately behind vehicle $j = 1$, both initially standing. This is the initial configuration. Then compute at every iteration step the joint PDF $P(d_1, v_1, d_2, v_2, t|d_0)$ which is the probability to find at time t vehicle $j = 1$ at a distance d_1 from vehicle $j = 0$ at velocity v_1, and to find vehicle $j = 2$ at a distance d_2 from vehicle $j = 1$ and velocity v_2. This joint PDF P is calculated iteratively from the initial conditions

$$P(d_1, v_1, d_2, v_2, 0|d_0) = \delta_{d_1, d_0} \delta_{v_1, 0} \delta_{d_2, 0} \delta_{v_2, 0}, \quad (4)$$

with $\delta_{a,b}$ the Kronecker delta. The time evolution of this PDF is determined by iteration rules that depend on different regimes of distances between the three vehicles. In the simplest case of sufficiently large distances, with the definition $P_{a,b} = P(d_1 + a, a, d_2 - a + b, b, t - 1|d_0)$, the iteration rule can be written as

$$P(d_1, v_1, d_2, v_2, t|d_0) = pp\,P_{v_1, v_2} + pq\,P_{v_1, v_2 - 1}$$
$$+ qp\,P_{v_1 - 1, v_2} + qq\,P_{v_1 - 1, v_2 - 1}, \quad (5)$$

with $q = 1 - p$. The precise form of the other iteration rules (5) slightly differ in the conditions on d_1, v_1, d_2, and v_2; and we refer for details to the Appendix. From this joint distribution, the PDF of a given variable is obtained by summing over all other variables. For instance, the velocity
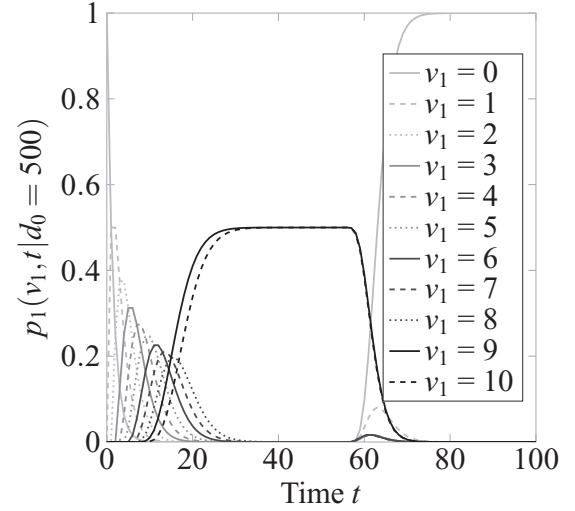

FIG. 6. Time evolution of the PDF $p_1(v_1, t|d_0)$ of vehicle 1 for all possible velocities and for an initial spacing $d_0 = 500$. We notice three distinct regimes in the time evolution of the probability to find vehicle 1 at velocity v_1. First the vehicle accelerates, corresponding to a decrease of the probability that it stands. Next, the occurrence of finite probabilities for intermediate velocities, signaling a transition to free flow with equally likely velocities $v_{\max} - 1$ and $v_{\max}$. Eventually, deceleration when vehicle 1 approaches the tail of the jam, corresponding to probability 1 to find the vehicle standing.

PDF $p_1(v_1, t|d_0)$ of vehicle $j = 1$ at time t reads as

$$p_1(v_1, t|d_0) = \sum_{d_1=0}^{d_0} \sum_{d_2=0}^{d_0} \sum_{v_2=0}^{v_{\max}} P(d_1, v_1, d_2, v_2, t|d_0). \quad (6)$$

The time evolution of this PDF for $d_0 = 500$ is plotted in Fig. 6 for all $v_{\max} + 1$ velocity states. From the probabilities for the different velocities v_1, we recognize three distinct phases: acceleration, free flow, and deceleration.

V. APPLICATION: RELATING HEADWAY AND VELOCITY DISTRIBUTIONS

In the previous section we developed an exact solution for PDFs within a 3-body approximation. We now investigate how this result can be used to link headway and velocity PDFs in the congested state. For this purpose, we base the reasoning on our observation that in a congested state the probability to find a standing vehicle is nonvanishing, see Sec. II. Therefore, if one takes a snapshot of a congested state at a given time, one observes standing vehicles with moving vehicles in between them. We start by focusing on these standing vehicles and the ones directly ahead of them, and hence on the constrained headway PDF of any stopped vehicle $Q_n(d_i|v_i = 0)$, and the constrained velocity PDF of any vehicle which is followed by a stopped vehicle $P_n(v_j|v_{j+1} = 0)$. While these two distributions can be obtained from our numerical simulation results with the NaSch model, we herein aim at obtaining an approximation $P_m(v_1|v_2 = 0)$ for this constrained velocity PDF within the 3-body approximation. We thus relate $P_m(v_1|v_2 = 0)$ to the numerically obtained headway PDF $Q_n(d_i|v_i = 0)$. By comparing the approximate to the numerically obtained velocity PDF, we can probe the accuracy
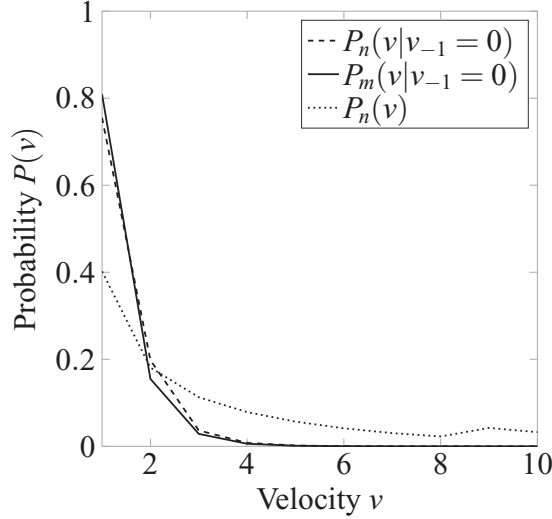
FIG. 7. Velocity PDFs P_n obtained numerically in the constrained and unconstrained case, and the velocity PDF P_m obtained from the headway distribution and the three-body approximation in the constrained case. The density is fixed at $\rho = 0.21$.

of the 3-body approximation. In order to relate the numerically computed headway distribution $Q_n(d_i|v_i = 0)$ to the 3-body approximation, we assume that a congested state can be described as a succession of 3-body blocks with a PDF $Q_0(d_0)$ for the initial spacing d_0. We define the summed probabilities

$$
\begin{aligned}
D_m(d_2, d_0) &= \sum_{t=0}^{T} \sum_{d_1=0}^{d_0} \sum_{v_1=0}^{v_{max}} P(d_1, v_1, d_2, 0, t|d_0), \\
V_m(v_1, d_0) &= \sum_{t=0}^{T} \sum_{d_1=0}^{d_0} \sum_{d_2=0}^{d_0} P(d_1, v_1, d_2, 0, t|d_0),
\end{aligned}
\tag{7}
$$

which can be viewed as matrices with row index d_2 (or v_1) and column index d_0. This allows us to express the headway distribution $Q_m(d_2|v_2 = 0)$ of vehicle 2 when it remains standing as

$$
Q_m(d_2|v_2 = 0) = D_m Q_0 = Q_n(d_i|v_i = 0). \tag{8}
$$

Similarly, we can easily obtain the velocity PDF of vehicles followed by a standing vehicle as

$$
P_m(v_1|v_2 = 0) = V_m Q_0 = V_m(D_m)^{-1} Q_n(d_i|v_i = 0). \tag{9}
$$

Note that the matrix D_m is invertible because it is triangular with nonvanishing diagonal elements. A comparison of the constrained velocity PDF obtained from simulations, $P_n(v_j|v_{j+1} = 0)$, and analytically with the 3-body approximation, $P_m(v_1|v_2 = 0)$, is plotted in Fig. 7 for a density of $\rho = 0.21$, and shows a fairly good agreement achieved without any adjustable fitting parameters. Noteworthy in this plot is the significant difference between the constrained and the unconstrained velocity PDFs, $P_n(v_j|v_{j+1} = 0)$ and $P_n(v)$, which underlines the limitations of mean-field theories. Note also that in order to keep the total iteration time T small enough, we use the velocity and headway distributions for moving vehicles only, i.e., excluding zero velocity and headway.

Next, we investigate how to relate the *unconstrained* velocity and headway PDFs that we obtained numerically, by using the 3-body approximation. To do so, one has to estimate the global headway PDF from the headway distributions of the two vehicles $j = 1, 2$ of the 3-body blocks. First, we define the headway PDFs as the matrices

$$
\begin{aligned}
\hat{D}_{m,1}(d, d_0) &= \sum_{t, v_1, d_2, v_2} P(d, v_1, d_2, v_2, t|d_0), \\
\hat{D}_{m,2}(d, d_0) &= \sum_{t, d_1, v_1, v_2} P(d_1, v_1, d, v_2, t|d_0).
\end{aligned}
\tag{10}
$$

Next, we introduce a parameter α to approximate the global headway distribution as a superposition of the ones for the two vehicles,

$$
\hat{D}_m = (1 - \alpha)\hat{D}_{m,1} + \alpha\hat{D}_{m,2}. \tag{11}
$$

Finally, we define the velocity PDFs

$$
\begin{aligned}
\hat{V}_{m,1} &= (v, d_0) = \sum_{t, d_1, d_2, v_2} P(d_1, v, d_2, v_2, t|d_0), \\
\hat{V}_{m,2} &= (v, d_0) = \sum_{t, d_1, v_1, d_2} P(d_1, v_1, d_2, v, t|d_0).
\end{aligned}
\tag{12}
$$

Since we have $\hat{V}_{m,1} \approx \hat{V}_{m,2}$, we will simply set $\hat{V}_m = \hat{V}_{m,1}$. We note that this approximation is justified since the velocity of vehicle $j = 2$ is essentially the same as the one of vehicle $j = 1$, but shifted in time. This does not hold for the headway distributions since the initial spacing between vehicles $j = 1$ and $j = 0$ is significantly different from the one between vehicles $j = 2$ and $j = 1$. Now we can use Eqs. (8) and (9) with D_m replaced by $\hat{D}_m$ and V_m replaced by $\hat{V}_m$ to obtain an approximation for the unconstrained velocity PDF $P(v)$ from the simulation result for the headway PDF $Q_n(d|v = 0)$. This approximation is now compared to the velocity PDF obtained from the simulations where α is used as a fitting parameter.

The results are shown in Fig. 8 for the choices $\alpha = 0$, $\alpha = 0.5$, and $\alpha = 0.95$ for a fixed density $\rho = 0.21$. One observes a remarkable agreement between the PDFs obtained from our numerical simulations and the 3-body approximation
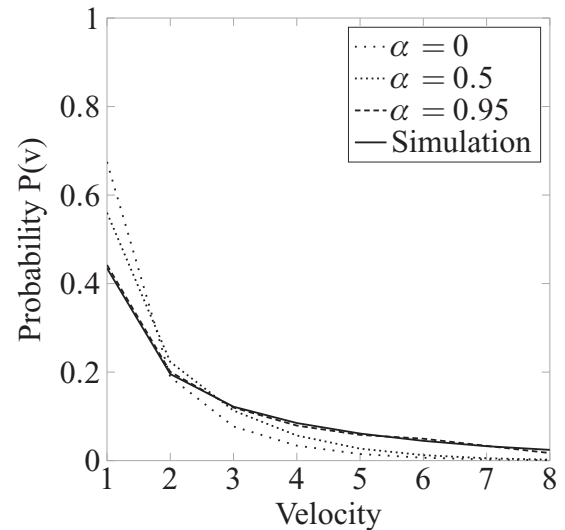

FIG. 8. Approximate results for the velocity PDF for different values of the fitting parameter α (dashed and dotted lines), and the velocity PDF obtained from simulations for a density $\rho = 0.21$.

applied to the simulation result for the headway distribution when the fitting parameter is $\alpha = 0.95$. The physical meaning of the fitting parameter, however, is not immediately obvious. A possible interpretation is the following. The basic assumption for the approximation presented here is that a congested state can be considered at any time step as a distribution of standing vehicles with moving vehicles in between them. In our 3-body approximation there is always a pair of moving vehicles ($j = 1, 2$) that approaches the tail of a jammed region (vehicle $j = 0$). Hence, one can view α as the relative importance of the distribution of the distance between the two vehicles of a pair, and $1 - \alpha$ as the relative importance of the distribution of the distance between a moving pair and the tail of the jam ahead. Our comparison in Fig. 8 then suggests that the velocity PDF in a jammed state is much more sensitive to the constrained distribution of the distances between two moving vehicles approaching a standing vehicle than the distribution of actual distances of the pair to the standing vehicle. This in turn suggests that the velocity PDF in a congested state is mostly determined by the dynamics within regions of still moving vehicles and not the interaction of these regions with jammed regions.

VI. CONCLUSION

In this paper we analyzed the statistics of velocities in the NaSch model. We studied the characteristics of the two phases and the phase transition in between them. We find that in the free flow phase the interactions between vehicles are negligible and that the velocity PDF assumes a simple form. The congested phase is characterized by a nonzero probability of finding a standing vehicle. We suggest using this probability as an approximate order parameter that might become a genuine order parameter in a continuum version of the model where $v_{\max} \to \infty$ velocity states exist. The nature of the phase transition could not be fully determined. There seems to be a discontinuity at a critical density but this could be an artefact of a too short simulation time. The velocity-velocity covariance function shows three different regimes: free flow with no correlation in velocity, a critical regime with diverging correlation number, and highly congested flow with a short correlation number. This scenario resembles a second-order phase transition.

Our simulations show that all PDFs are highly dependent on the density, whether in free flow or in the completely congested regime, with the exception of a simple PDF for the velocities in the low-density free flow. We presented an analytical solution for a 3-body approximation, that allowed us to analytically link the headway and velocity distribution functions. We first focused on a constrained case with stopped vehicles, and then studied the unconstrained case. This approximation describes nicely the constrained case. By introducing a fitting parameter in the constrained case, we could also reach a remarkable agreement between simulation results and our approximation. An attempt to interpret the physical meaning of the fitting parameter has been made. However, the dependence of this fitting parameter on the values of $v_{\max}$ and p have not been studied and are left to future work. Pushing the method presented in this paper could prove useful, possibly enabling one to link headway and velocity as well as other quantities of interest and to learn more about the local dynamics in the jammed phase.

In addition to offering a perspective on traffic models, the present study of velocity statistics might help identify the nature of a potential phase transition in the stochastic NaSch model. Moreover, in more applied terms, the knowledge of velocity distributions enables one to compute expected excess fuel consumption related to road properties as the ones studied in Refs. [9–11] as a function of traffic conditions, which is the topic of a forthcoming paper. This relation opens new perspectives, alongside with the recent boom of data collections [12], which enables one to revisit traffic models and adapt them to meet the requirements of other research areas such as carbon management.

APPENDIX: DETAILS OF THE 3-BODY APPROXIMATION

To obtain the complete iteration rules of the 3-body interaction approximation we introduce the notion of *limiting speed* $\hat{v}_j = \min(d_j, v_{\max})$, which is the speed that the vehicle j cannot exceed at any given time. For each vehicle we have to distinguish three cases: (i) $v_j < \hat{v}_j - 1$, (ii) $v_j = \hat{v}_j - 1$, and (iii) $v_j = \hat{v}_j$, with the assumption that $d_j > 1$, the case $d_j = 0$ being trivial. The indices 1 and 2 being interchangeable, we denote six different cases:

(1) $v_1 < \hat{v}_1 - 1$ and $v_2 < \hat{v}_2 - 1$,
(2) $v_1 = \hat{v}_1 - 1$ and $v_2 < \hat{v}_2 - 1$,
(3) $v_1 = \hat{v}_1$ and $v_2 < \hat{v}_2 - 1$,
(4) $v_1 = \hat{v}_1 - 1$ and $v_2 = \hat{v}_2 - 1$,
(5) $v_1 = \hat{v}_1$ and $v_2 = \hat{v}_2 - 1$,
(6) $v_1 = \hat{v}_1$ and $v_2 = \hat{v}_2$.

Finally we introduce the scalar variables

$$r_j = \begin{cases} p & \text{if } v_j < \hat{v}_j \\ q & \text{if } v_j = \hat{v}_j \end{cases}; \quad s_j = \begin{cases} q & \text{if } v_j > 0 \\ 0 & \text{if } v_j = 0 \end{cases}. \quad \text{(A1)}$$

With that in hand we write the iteration rule for all the cases. Case (1) is the most simple and given in Eq. (5). Cases (2) and (3) can be grouped together and follow the iteration rule

$$P = r_1 \sum_{w_1=v_1}^{v_{\max}} \left(r_2 P_{w_1, v_2} + s_2 P_{w_1, v_2-1} \right) + s_1 r_2 P_{v_1-1, v_2} + s_1 s_2 P_{v_1-1, v_2-1}, \quad \text{(A2)}$$

with $P = P(d_1, v_1, d_2, v_2, t | d_0)$. As for cases (4)–(6), they also can be grouped in the same iteration rule, in the form

$$P = r_1 \sum_{w_1=v_1}^{v_{\max}} \left(r_2 \sum_{w_2=v_2}^{v_{\max}} P_{w_1, w_2} + s_2 P_{w_1, v_2-1} \right) + s_1 r_2 \sum_{w_2=v_2}^{v_{\max}} P_{v_1-1, w_2} + s_1 s_2 P_{v_1-1, v_2-1}. \quad \text{(A3)}$$

Implementing these iteration rules numerically is tedious but not technically difficult, and enables one to retrieve the results described in Sec. IV.

[1] A. Schadschneider, D. Chowdhury, and K. Nishinari, *Stochastic Transport in Complex Systems: From Molecules to Vehicles* (Elsevier, Philadelphia, 2010).

[2] D. Chowdhury, L. Santen, and A. Schadschneider, Phys. Rep. **329**, 199 (2000).

[3] M. Gerwinski and J. Krug, Phys. Rev. E **60**, 188 (1999).

[4] K. Nagel and M. Schreckenberg, J. Phys. I **2**, 2221 (1992).

[5] M. Schreckenberg, A. Schadschneider, K. Nagel, and N. Ito, Phys. Rev. E **51**, 2939 (1995).

[6] R. Barlovic, L. Santen, A. Schadschneider, and M. Schreckenberg, Eur. Phys. J. B **5**, 793 (1998).

[7] S. Lübeck, M. Schreckenberg, and K. D. Usadel, Phys. Rev. E **57**, 1171 (1998).

[8] S. Krauss, P. Wagner, and C. Gawron, Phys. Rev. E **54**, 3707 (1996).

[9] A. Louhghalam, M. Akbarian, and F.-J. Ulm, J. Eng. Mech. **140**, 04014053 (2013).

[10] A. Louhghalam, M. Akbarian, and F.-J. Ulm, Transp. Res. Rec. **2457**, 95 (2014).

[11] A. Louhghalam, M. Akbarian, and F.-J. Ulm, in Transportation Research Board 94th Annual Meeting, 2015 (unpublished).

[12] M. Fazeen, B. Gozick, R. Dantu, M. Bhukhiya, and M. C. González, IEEE Trans. Intell. Transport. Syst. **13**, 1462 (2012).